

Relationship between urate within tophus and bone erosion according to the anatomic location of urate deposition in gout

A quantitative analysis using dual-energy CT volume measurements

Dan Shi, MD^a, Jie-Yu Chen, MD^a, Hua-Xiang Wu, MD^b, Qi-Jing Zhou, MD^a, Hai-Yan Chen, MD^a, Yuan-Fei Lu, MD^a, Ri-Sheng Yu, MD, PhD^{a,*}

Abstract

The aim of this study was to measure the urate volume within tophus and bone erosion volume using dual-energy computed tomography in patients with tophaceous gout. Furthermore, our study aims to quantitatively analyze the relationship between monosodium urate (MSU) crystal deposition and bone erosion according to the anatomic location of urate deposition.

Seventy-seven subjects with chronic gout were positively identified for the presence of urate deposition. Only 27 subjects identified for the presence of urate in contact with bone erosion were included in this study. The urate volumes and associated erosion volumes were measured. The relationships between urate within tophus and bone erosion were separately analyzed according to the anatomic location of urate deposition.

Twenty-seven subjects were all male (100%) with a median (interquartile range, IQR) age of 52 (45–61) years. From all the subjects, 103 tophi depositions were identified in contact with bone erosion, including 58/103 tophi that contained an intraosseous component and 45/103 nonintraosseous tophi. Tophi containing intraosseous components were larger than nonintraosseous tophi (urate volume: median [IQR] 45.64 [4.79–250.89] mm³ vs 19.32 [6.97–46.71] mm³, $P = .035$) and caused greater bone erosion (erosion volume: 249.03 [147.08–845.33] mm³ vs 69.07 [32.88–111.24] mm³, $P < .001$). Almost all erosion volumes were larger than urate volumes in nonperiarticular tophi, in contrast to most erosion volumes, which were less than urate volumes in the tophi that contained a periarticular component (odds ratio, 95% confidence interval: 74.00, 14.70–372.60; $P < .001$). Urate volume and erosion volume demonstrated positive correlations in intraosseous tophi, intraosseous-intra-articular-periarticular tophi, and intraosseous-intra-articular tophi ($r_s = 0.761$, $r_s = 0.695$, $r_s = 0.629$, respectively, $P < .05$).

MSU crystal deposition shows a promoting effect on the development of bone erosions in varying degrees, associated with the location of MSU crystals deposited in the joints. The intraosseous tophi contribute the most to bone erosions, followed by intra-articular tophi, and periarticular tophi.

Abbreviations: BMO = bone marrow edema, CI = confidence interval, CRP = C-reactive protein, DECT = dual-energy computed tomography, ESR = erythrocyte sedimentation rate, IQR = interquartile range, MSU = monosodium urate, OR = odds ratio.

Keywords: dual-energy computed tomography, erosion, gout, quantitative analysis, tophus

Editor: Qinhong Zhang.

The authors have no conflicts of interest to disclose.

^aDepartment of Radiology, ^bDepartment of Rheumatology, The Second Affiliated Hospital, Zhejiang University School of Medicine, Hangzhou, China.

*Correspondence: Ri-Sheng Yu, Department of Radiology, The Second Affiliated Hospital, Zhejiang University School of Medicine, Jiefang Road 88#, Hangzhou 310009, China (e-mail: risheng-yu@zju.edu.cn).

Copyright © 2019 the Author(s). Published by Wolters Kluwer Health, Inc. This is an open access article distributed under the terms of the Creative Commons Attribution-Non Commercial License 4.0 (CCBY-NC), where it is permissible to download, share, remix, transform, and buildup the work provided it is properly cited. The work cannot be used commercially without permission from the journal.

How to cite this article: Shi D, Chen JY, Wu HX, Zhou QJ, Chen HY, Lu YF, Yu RS. Relationship between urate within tophus and bone erosion according to the anatomic location of urate deposition in gout: A quantitative analysis using dual-energy CT volume measurements. *Medicine* 2019;98:51(e18431).

Received: 8 February 2019 / Received in final form: 20 October 2019 /

Accepted: 14 November 2019

<http://dx.doi.org/10.1097/MD.00000000000018431>

1. Introduction

Gout is the most common inflammatory arthritis in men and has a rapidly expanding prevalence in the general population.^[1] The contemporary prevalence of gout is 3% to 6% in men and 1% to 2% in women in western developed countries.^[2] In the Shandong coastal cities of Eastern China, the prevalence in 2008 was estimated to be 1.14% in adults.^[2] Gout is characterized by the deposition of monosodium urate (MSU) crystals in cartilage, joints, and soft tissues, and occurs due to long-standing hyperuricemia.^[3] Tophus, the hallmark of chronic gout, is a high-density soft tissue nodule, which represents a chronic granulomatous response to MSU crystals.^[4] Tophaceous deposits can erode into the bone, cartilage, and tendons, causing significant structural damage.^[5–7] The process underlying the development of bone erosions in chronic gout remains unclear. Collectively, most imaging observations support the concept that MSU crystals deposit on the surface of articular cartilage, or within the synovium, and subsequently interact with bone cells to

develop erosions. This is the most accepted mechanism for the development of bone erosion and joint damage in gout.^[8–11] However, previous studies have not explored whether the anatomic location of MSU crystal deposition correlates to the effects of MSU crystals to promote bone erosions.

It is hard to distinguish MSU crystals from chronic granulomatous tissue. Tophus volumes measured by previous methods all include both uric acid crystals and noncrystal components.^[8,12,13] The direct role of MSU crystals in the development of bone erosions in gout has not been examined using three-dimensional volume measurements. Dual-energy computed tomography (DECT) has the inherent capability to distinguish urate from calcific mineralization, and can quantify only MSU crystal elements through an automated volume estimation procedure.^[14] The mixed images of DECT can achieve a similar or improved quality compared with the typical 120-kVp single-energy scans,^[15] which is considered as a standard reference with a superior ability compared to both radiography and magnetic resonance imaging when detecting bone erosions in rheumatoid arthritis^[16,17] and chronic gout.^[8]

The objective of this study was to quantitatively analyze the relationship between MSU crystal deposition and bone erosion according to the anatomic location of urate deposition of the joints (intraosseous tophus, intra-articular tophus, and periarticular tophus), using DECT in patients with tophaceous gout. Specifically, we wish to determine whether intraosseous tophi, intra-articular tophi, and periarticular tophi have an impact on bone erosion of varying degrees.

2. Materials and methods

2.1. Patients

This is a retrospective study of patients with chronic gout recruited from the Outpatient Rheumatology Clinic in our hospital, Hangzhou, China, from June 2010 to February 2015. All patients were diagnosed as gout based on the 1977 American Rheumatism Association classification criteria, and required at least 1 palpable tophus to be reported on clinical examination.^[18] All patients proceeded to DECT scanning of their feet. Women of childbearing age, patients with acute gout flares at the time of assessment, diabetes mellitus patients, or patients with lower limb amputations were excluded from the study. Approval by the local ethics committee was obtained and a signed informed consent was provided by all patients. The clinical characteristics related to gout were recorded, including age, gender, disease duration, serum uric acid, C-reactive protein (CRP), and erythrocyte sedimentation rate (ESR). Blood samples were obtained on the day of DECT scanning.

2.2. DECT scanning

DECT scans were performed at the Radiology Department using the second-generation 128-slice dual source CT scanner (Somatom Definition Flash; Siemens Healthcare, Forchheim, Germany). Scanning started 5 cm proximal to the ankles and was directed toward the tip of the patient's toes, in a craniocaudal direction. Patients were positioned in a supine position with the feet in a plantar flexion position. The DECT system was equipped with 2 X-ray tubes, which were angled at 95° to one another on a gantry and could rotate simultaneously at different energies (e.g., 80 kV and 140 kV). The 2 data sets were loaded into a

postprocessing software (Dual Energy, Syngo CT Workplace, Siemens Healthcare) on the Syngo multimodality workstation (SW-Version VA20, Siemens Healthcare). Soft tissue portions of the images were used as the baseline: materials above the baseline were color-coded in green (uric acid), and below the baseline were color-coded in purple (calcium) (Fig. 1A). The images reconstructed from different energies scans (typically at 80 and 140 kV, respectively) could be mixed together to provide a single set of nonmaterial specific images for routine diagnostic interpretation^[15] (Fig. 1B). The composition ratio of mixed images was 0.4, by using the following formula: $HU_{w-av} = 0.4HU_{80-kVp} + 0.6HU_{140-kVp}$, where HU_{w-av} is Hounsfield units on the mixed images, HU_{80-kVp} is Hounsfield units on 80 kVp images and $HU_{140-kVp}$ is Hounsfield units on 140 kVp images. The following scanning parameters were used: 80 kV and 250 mAs for tube A; 140 kV and 125 mAs for tube B; collimation of 0.6 mm reconstructed to 0.75 mm transverse thick slices.

2.3. Urate volume and erosion volume measurements

Two trained musculoskeletal radiologists (D.S. and R.-S.Y.) who were experienced in evaluating DECT images independently scored all individual joints of feet (52 joints available for scoring from each patient). The axial, sagittal, and coronal images were viewed to confirm bone erosion, which was defined as a focal area of loss of the cortex with sharply defined margins along 2 planes, as well as the presence of a breach of the bone cortex in at least 1 plane. Each site was first scored for the presence or absence of MSU crystal deposition and bone erosion. If urate was present adjacent to or within the joint, the presence of urate in contact with bone erosion was then scored. Only patients were identified for the presence of urate in contact with bone erosion were included in this study. For urate in contact with bone erosion, the site was then scored in regards to the presence of urate within an erosion and if not within an erosion, adjacent to the erosion only.

According to the anatomic location of urate deposition: for those tophi that showed urate deposition within the erosion (tophi containing intraosseous components), they were classified into intraosseous tophi (urate deposition only within the erosion), intraosseous-intra-articular tophi (urate deposition was regarded as 2 parts: deposition within the erosion and within the joint), and intraosseous-intra-articular-periarticular tophi (urate deposition was regarded as 3 parts: deposition within the erosion, within the joint, and adjacent to the joint); for those tophi that showed urate deposition within the joint and adjacent to the erosion (nonintraosseous tophi), but not extending into the erosion, they were classified into intra-articular tophi (urate deposition only within the joint), and intra-articular-periarticular tophi (urate deposition was regarded as 2 parts: deposition within the joint and adjacent to the joint).

When readers differed, the score was decided by consensus. Urate volume of each index tophus was quantified by circling the tophus regions (Fig. 1C) and total urate volume per patient was quantified by circling the entire bodily regions, using an automated volume assessment software (volume @ syngo MMWP VE 40A 2010; Siemens Healthcare, Forchheim, Germany). Using the same volume assessment software, each erosion volume was measured manually by drawing freehand around their margins on all axial slices of the mixed images (Fig. 1D). The total erosion volume per patient was calculated by adding all individual erosion volumes reported in each patient.

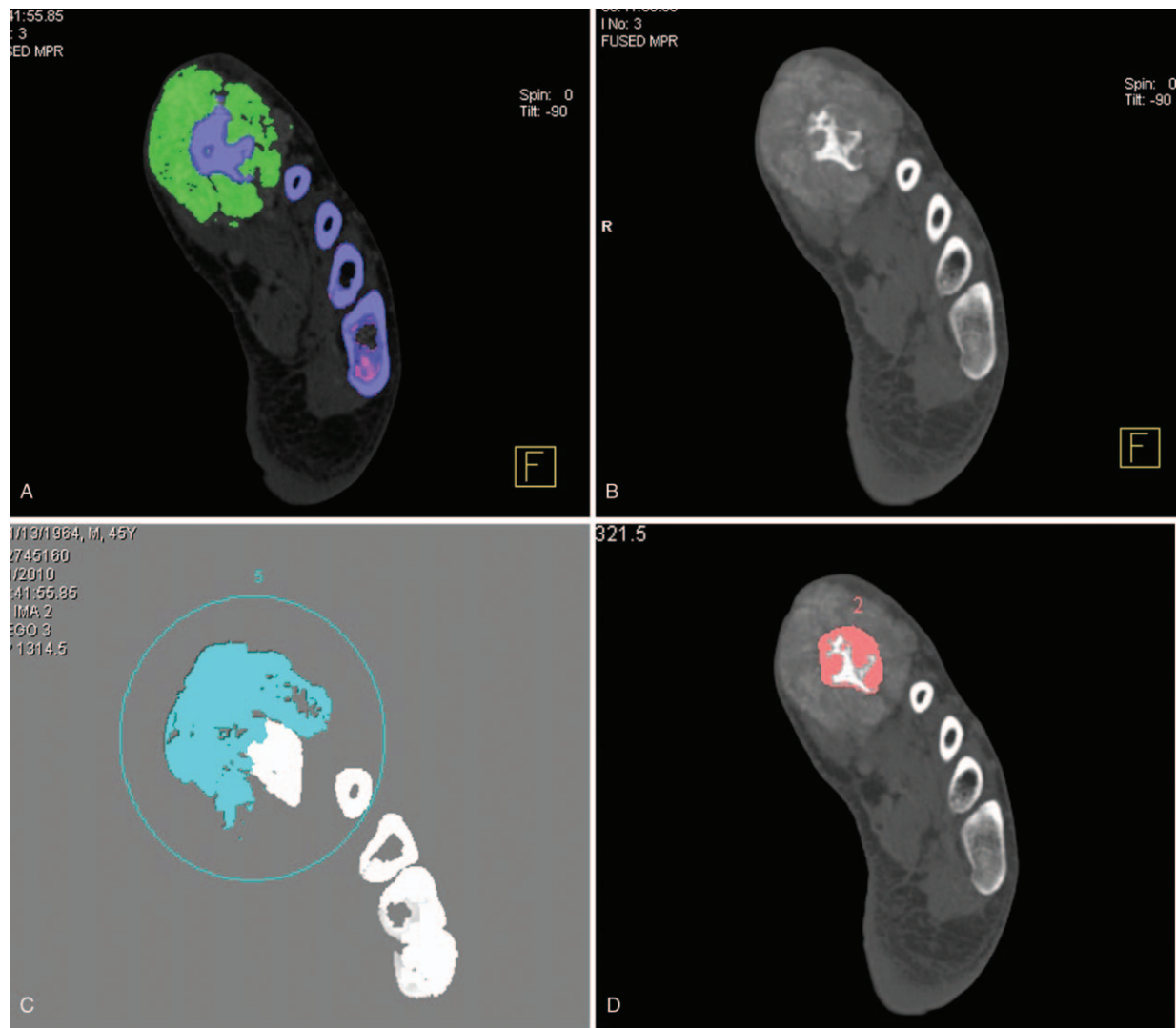


Figure 1. Dual energy computed tomography (DECT) images of a 45-year-old man with chronic tophaceous gout showing uric acid deposits in contact with bone erosion. With the application of the 3-material decomposition algorithm, uric acid deposits were depicted in green, whereas calcium deposition in the bone was depicted in purple: (A) axial color-coded DECT 2-material decomposition images illustrating intraosseous-intra-articular-periarticular tophus at the first metatarsophalangeal joint; (B) tophus and bone erosion presented on mix images; (C) urate volume was automatically calculated by circling the entire forefoot area; (D) erosion volume was automatically calculated by circling the rim of entire erosion.

Our previous study demonstrated a high reproducibility of urate volume and erosion volume measurements using DECT.^[19] The mean urate volume and erosion volume were recorded for each site. The intraclass correlation coefficient (95% confidence interval [CI]) for urate volume and erosion volume measurement was 1.000 (1.000, 1.000), 0.999 (0.998, 0.999), respectively.

2.4. Statistical analysis

Statistical Package for the Social Sciences for Windows, version 20 (SPSS, Chicago, IL) was used for statistical analysis. Clinical characteristics: urate volumes and erosion volumes were described using medians with interquartile ranges (IQRs), or percentages. Differences between groups were analyzed using nonparametric tests, and Chi-squared analysis or Fisher exact test with calculation of odds ratios (ORs) with 95% CIs. Spearman Rho correlation coefficients (r_s) described the associations between variables. Linear regressions were used to analyze the

relationships between urate within tophus and bone erosion. All tests were two-tailed at the 0.05 significant levels.

3. Results

3.1. Patient and clinical characteristics

Seventy-seven patients were positively identified for the presence of urate deposition (2 patients were scanned twice). Of the 77 patients, 27 (35%) showed at least 1 tophus deposition in contact with bone erosion. The median (IQR) age of the 27 subjects was 52 (45–61) years and 27 (100%) were male patients. The median (IQR) gout disease duration was 84 (48–120) months. The median (IQR) number of total tophi per patient was 14 (8–20). The median (IQR) serum uric acid, CRP, and ESR were 0.48 (0.41–0.64) mmol/L (8.1 [6.9–10.8] mg/dL), 15.2 (9.6–25.7) mg/L, and 10 (6–37) mm/hours, respectively (Table 1). No significant correlation was demonstrated between the total urate volume or

Table 1**Clinical characteristics of study participants (n=27).**

| | |
|--------------------------------|--|
| Male sex, n (%) | 27 (100%) |
| Age, median (IQR) | 52 (45–61) years |
| Disease duration, median (IQR) | 84 (48–120) months |
| Number of tophi, median (IQR) | 14 (8–20) |
| Serum uric acid, median (IQR) | 0.48 (0.41–0.64) mmol/L (8.1 [6.9–10.8] mg/dL) |
| CRP, median (IQR) | 15.2 (9.6–25.7) mg/L |
| ESR, median (IQR) | 10 (6–37) mm/h |

CRP=C-reactive protein, ESR=erythrocyte sedimentation rate, IQR=interquartile range, n=number.

total erosion volume, and age, serum uric acid, CRP, or ESR (data not shown). The disease duration demonstrated a positive correlation with the total erosion volume ($r_s=0.493$, $P=.032$); however, this correlation was not demonstrated for the total urate volume ($r_s=0.253$, $P=.296$). There were significant correlations between the number of total tophi and total urate volume ($r_s=0.554$, $P=.003$), as well as total erosion volume ($r_s=0.455$, $P=.017$).

3.2. Comparison of urate volume and erosion volume according to the anatomic location of urate deposition

For all individual joints assessed, urate deposition adjacent to or within the joint was present in 399 (28.4%) of 1404 joints from all 27 subjects. For those tophi deposited adjacent to or within the joints, 6 tophi were observed deposited in more than 1 joint (range 2–4 joints). Each tophus was regarded as an independent unit for volume measurement. Finally, there were 387 tophi for statistical analysis. Bone erosions were present in 225 (16.0%) of 1404 joints. The median (IQR) urate volume and erosion volume were 6.99 (1.77–27.22) mm³ and 106.07 (43.62–237.51) mm³. For those tophi identified, urate deposition in contact with erosion was present in 104 (26.9%) of 387 tophi. Twenty-seven tophi were in contact with more than 1 erosion (range 2–5 erosions), and 1 erosion was in contact with 2 tophi. For the purposes of the site-by-site analysis, each tophus/erosion was initially considered as an independent unit (1 tophus to 1 erosion) by adding the volumes and was then finally processed as 103 tophi/erosions for the statistical analysis (Fig. 2).

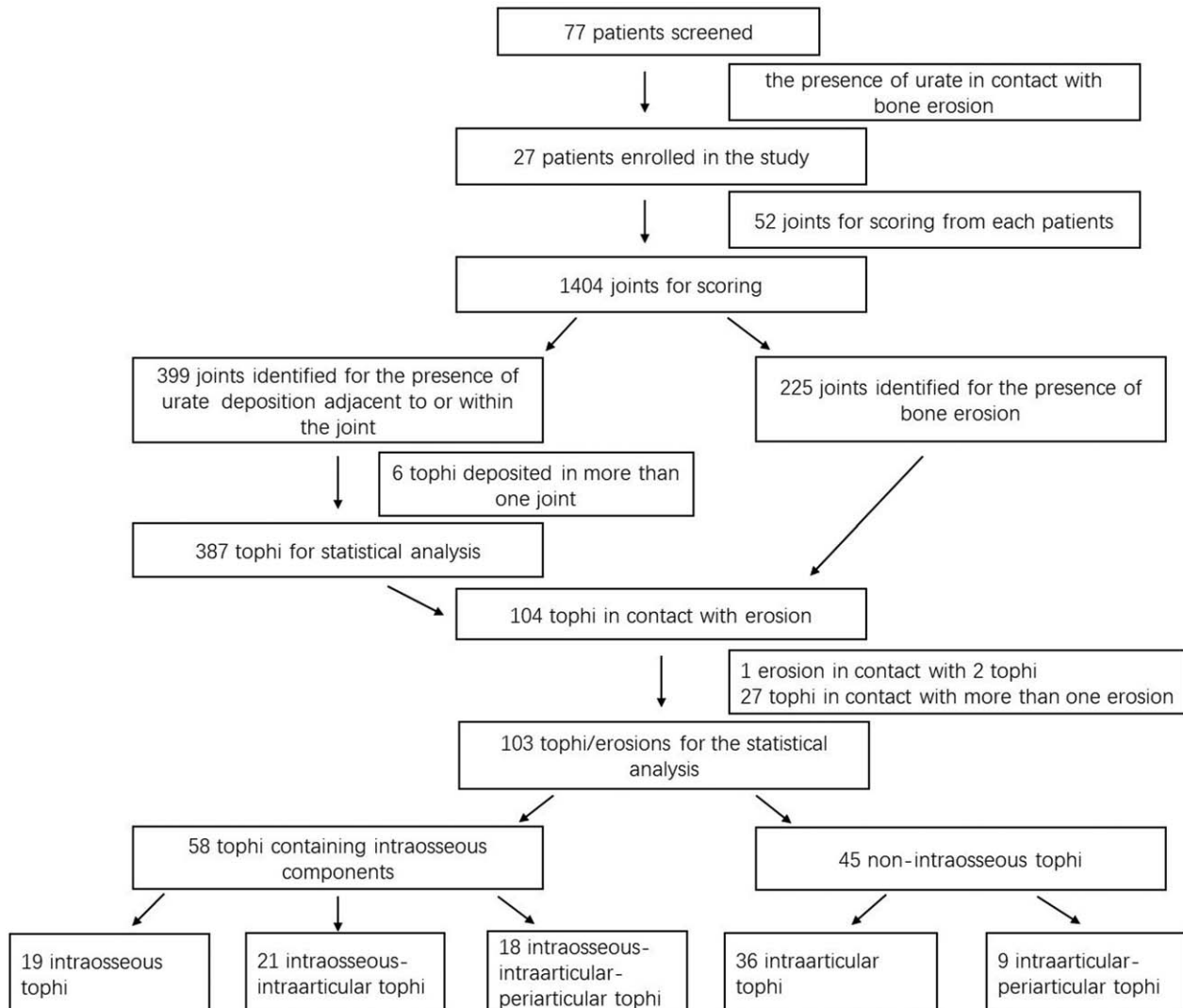


Figure 2. Flow diagram of the number of tophi and joints assessed through the study.

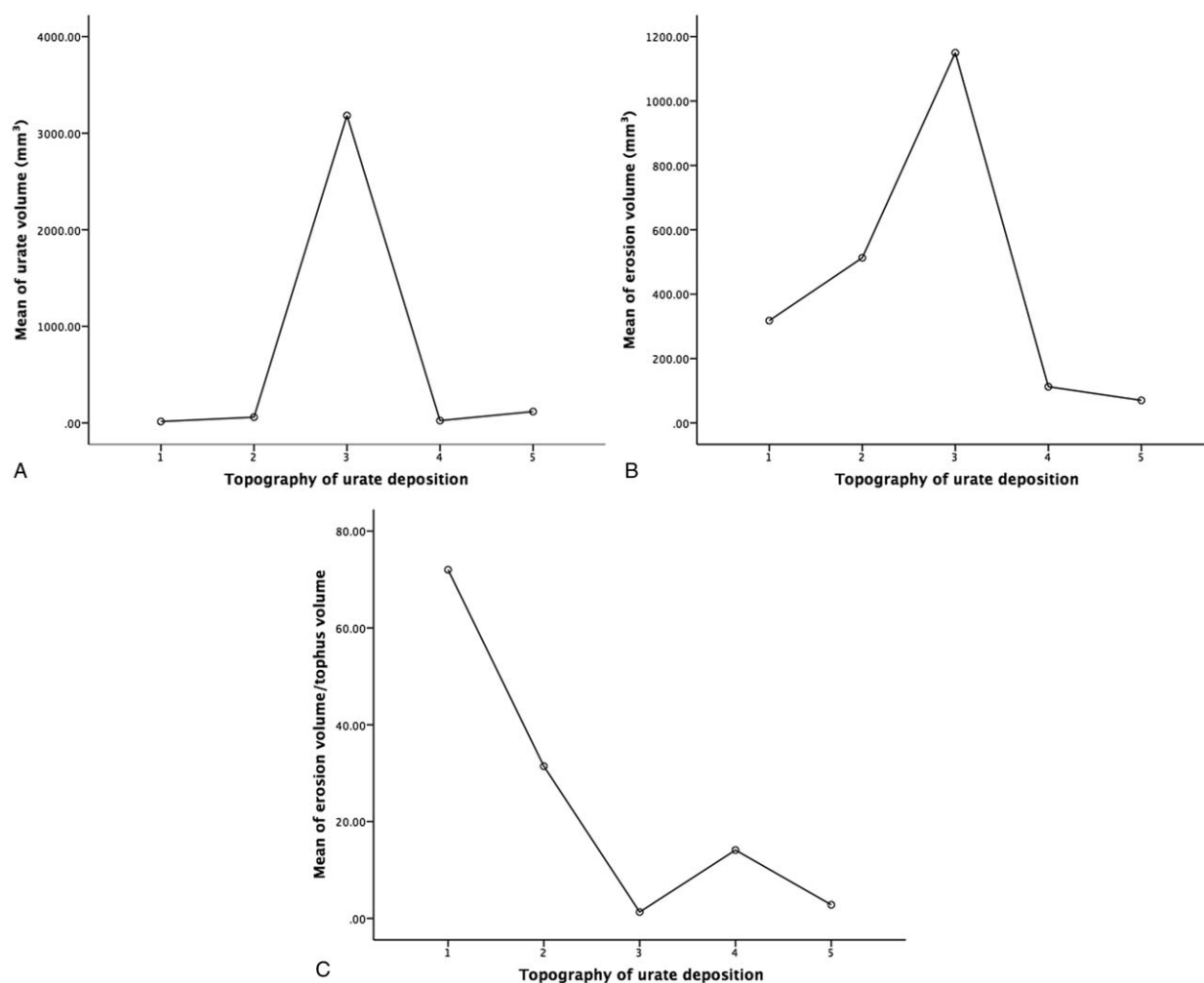


Figure 3. Mean plot showed the trend of urate volume, erosion volume, and erosion volume/urate volume according to the anatomic location of tophus deposition: (A) mean of urate volume; (B) mean of erosion volume; (C) mean of erosion volume/urate volume. 1 = intraosseous tophi, 2 = intraosseous-intra-articular tophi, 3 = intraosseous-intra-articular-periarticular tophi, 4 = intra-articular tophi, 5 = intra-articular-periarticular tophi.

There were 58/103 (56.3%) tophi that contained an intraosseous component, including 19/58 (32.8%) intraosseous tophi, 21/58 (36.2%) intraosseous-intra-articular tophi, and 18/58 (31.0%) intraosseous-intra-articular-periarticular tophi. There were 45/103 (43.7%) nonintraosseous tophi, including 36/45 (80.0%) intra-articular tophi, and 9/45 (20.0%) intra-articular-periarticular tophi. Individual periarticular tophus that in contact with bone was not observed at any site. Tables 2 and 3 show the descriptive and difference analyses of urate volume and erosion volume according to the anatomic location of urate deposition (Fig. 3). Tophi containing intraosseous components were larger than nonintraosseous tophi and resulted in greater bone erosion.

There were 76 nonperiarticular tophi, 74/76 erosion volumes that were larger than urate volumes and 2/76 erosion volumes less than urate volumes. This was compared to 9/27 erosion volumes that were larger than urate volumes and 18/27 erosion volumes less than urate volumes for tophi that contained the periarticular component (OR, 95%CI: 74.00, 14.70–372.60; $P < .001$) (Table 4).

3.3. Relationship between urate volume and erosion volume according to the anatomic location of urate deposition

Strong positive correlations were demonstrated between urate volume and erosion volume in the intraosseous tophi ($r_s = 0.761$, $P < .001$) (Fig. 4A), intraosseous-intra-articular-periarticular tophi ($r_s = 0.695$, $P = .001$) (Fig. 4B), and intraosseous-intra-articular tophi ($r_s = 0.629$, $P = .002$) (Fig. 4C). For those tophi that contained an intraosseous component, similar correlations were demonstrated ($r_s = 0.651$, $P < .001$). The correlation in the intra-articular tophi was weaker ($r_s = 0.431$, $P = .009$). No significant correlation was demonstrated in the intra-articular-periarticular tophi ($r_s = 0.217$, $P = .576$) (Table 2).

The median (IQR) total urate volume and total erosion volume per patient was 360.32 (116.52–1304.06) mm³ and 624.51 (241.18–3873.79) mm³. There was a positive correlation noted between the total urate volume and total erosion volume per patient ($r_s = 0.670$, $P < .001$).

Table 2

Summary of dual-energy computed tomography volume measurements, and the relationship between urate volume and erosion volume according to the anatomic location of urate deposition.

| Site | Urate volume | Erosion volume | Erosion volume/ | Correlations between urate volume and erosion volume* |
|---|-------------------------------------|-------------------------------------|-------------------------------|--|
| | (mm ³) median IQR | (mm ³) median IQR | urate volume median IQR | |
| Tophi containing intraosseous components (n=58) | 45.64 4.79–250.89 | 249.03 147.08–845.33 | 8.24 2.28–25.75 | $r_s = 0.651$ $P < .001^\dagger$ |
| Intraosseous tophi (n=19) | 2.87 0.94–22.31 | 194.27 55.48–375.03 | 31.83 16.97–77.14 | $r_s = 0.761$ $P < .001^\dagger$ |
| Intraosseous-intra-articular tophi (n=21) | 36.86 13.11–108.00 | 241.18 184.18–486.90 | 9.44 3.71–22.56 | $r_s = 0.629$ $P = .002^\dagger$ |
| Intraosseous-intra-articular-periarticular tophi (n=18) | 625.16 294.70–1688.57 | 793.23 198.67–1332.41 | 0.74 0.40–2.15 | $r_s = 0.695$ $P = .001^\dagger$ |
| Nonintraosseous tophi (n=45) | 19.32 6.97–46.71 | 69.07 32.88–111.24 | 3.78 1.22–14.14 | $r_s = 0.202$ $P = .184$ |
| Intra-articular tophi (n=36) | 16.12 4.59–31.17 | 73.02 43.88–116.30 | 5.52 2.36–17.73 | $r_s = 0.431$ $P = .009^\dagger$ |
| Intra-articular-periarticular tophi (n=9) | 101.77 28.94–128.30 | 34.11 26.38–92.68 | 0.60 0.22–1.75 | $r_s = 0.217$ $P = .576$ |

DECT = dual-energy computed tomography, IQR = interquartile range, n = number.

* Values represent Spearman Rho correlation coefficients.

† Statistically significant results.

Table 3

Comparison of urate volume and erosion volume according to the anatomic location of urate deposition.

| Difference analyses | P | | |
|---|--------------|----------------|-----------------------------|
| | Urate volume | Erosion volume | Erosion volume/urate volume |
| Tophi containing intraosseous components and nonintraosseous tophi | $P = .035^*$ | $P < .001^*$ | $P = .125$ |
| Intraosseous tophi and intraosseous-intra-articular tophi | $P = .014^*$ | $P = .112$ | $P = .019^*$ |
| Intraosseous tophi and intraosseous-intra-articular-periarticular tophi | $P < .001^*$ | $P = .007^*$ | $P < .001^*$ |
| Intraosseous-intra-articular tophi and intraosseous-intra-articular-periarticular tophi | $P < .001^*$ | $P = .235$ | $P < .001^*$ |
| Intra-articular tophi and intra-articular-periarticular tophi | $P = .002^*$ | $P = .173$ | $P = .001^*$ |

Difference analyses using nonparametric tests.

* Statistically significant results.

4. Discussion

In prior laboratory and imaging studies, tophus infiltration into underlying bone represents the dominant mechanism for the development of joint damage in gout.^[8,20] For the marked variation in MSU crystal content within tophi, it cannot be assumed that the previously observed relationship between tophi

and structural joint damage is directly due to the effects of MSU crystal deposition.^[9] The use of DECT has enabled noninvasive visualization of MSU crystal deposition within areas of bone erosion and has provided a new insight into this question. In 1 recent DECT study,^[9] researchers have reported that MSU crystals are frequently present in joints affected by radiographic

Table 4

Comparison between erosion volume and urate volume according to the anatomic location of urate deposition.

| Site | Erosion volume > urate volume | Erosion volume < urate volume | OR (95% CI) | P |
|---|-------------------------------|-------------------------------|----------------------|--------|
| Tophi containing intraosseous components (n=58) | 47 (46.7) | 11 (11.3) | 1.07 (0.40–2.85) | .895 |
| Nonintraosseous tophi (n=45) | 36 (36.3) | 9 (8.7) | | |
| Nonperiarticular tophi (n=76) | 74 (61.2) | 2 (14.8) | 74.00 (14.70–372.60) | <.001* |
| Tophi containing periarticular components (n=27) | 9 (21.8) | 18 (5.2) | | |
| Intraosseous tophi (n=19) | 19 (13.4) | 0 (5.6) | 2.57 (1.44–4.59) | <.001* |
| Intraosseous-intra-articular-periarticular tophi (n=18) | 7 (12.6) | 11 (5.4) | | |
| Intraosseous-intra-articular tophi (n=21) | 21 (15.1) | 0 (5.9) | 2.57 (1.44–4.59) | <.001* |
| Intraosseous-intra-articular-periarticular tophi (n=18) | 7 (12.9) | 11 (5.1) | | |
| Intra-articular tophi (n=36) | 34 (28.8) | 2 (7.2) | 59.50 (7.13–496.74) | <.001* |
| Intra-articular-periarticular tophi (n=9) | 2 (7.2) | 7 (1.8) | | |

Odds ratio (OR) with 95% confidence interval (CI) calculated with Chi-squared analysis or Fisher exact test.

CI = confidence interval, n = number, OR = odds ratio.

* Statistically significant results.

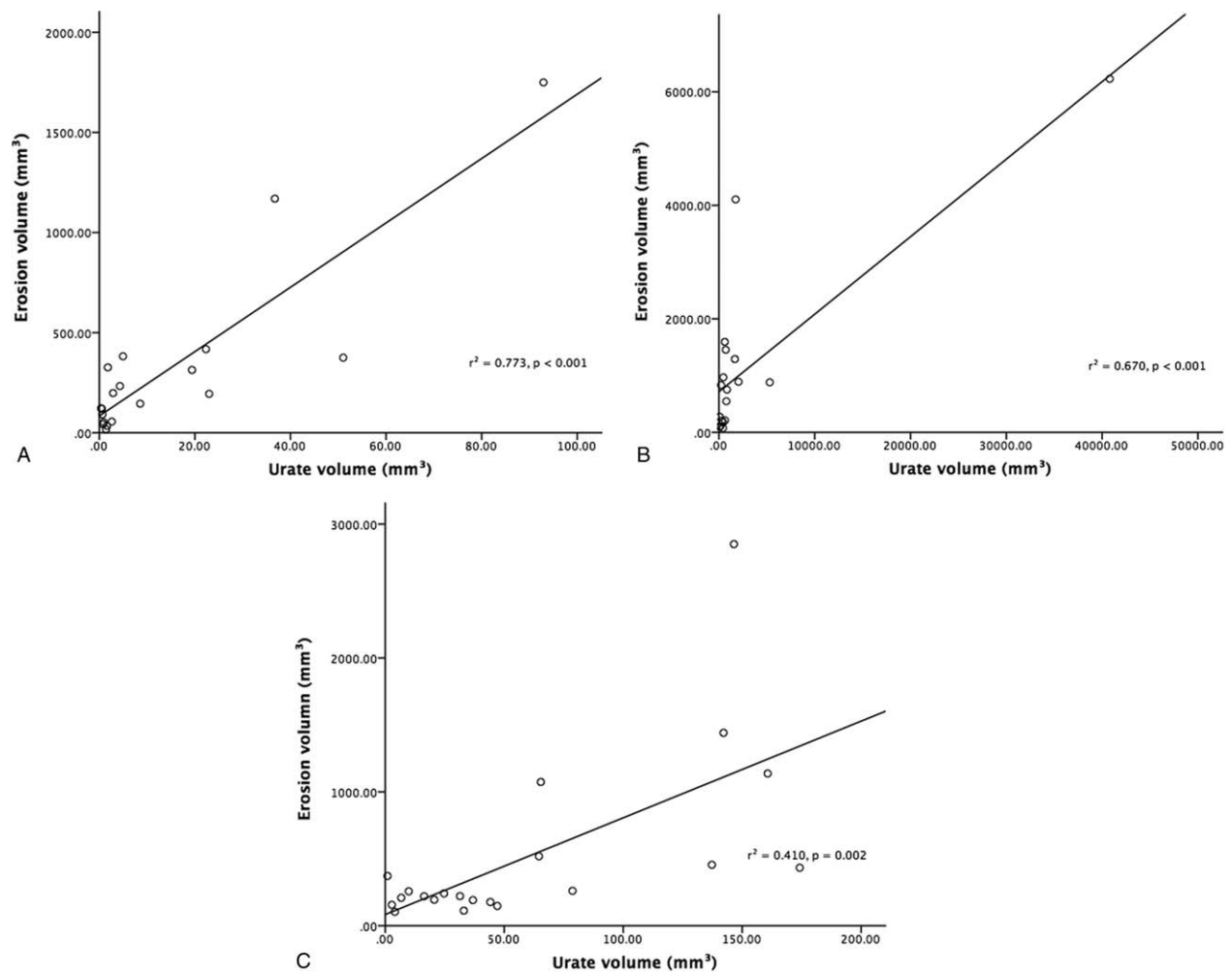


Figure 4. Relationship between urate volume and erosion volume according to the anatomic location of tophus deposition. Linear regression was shown in all graphs: (A) intraosseous tophi, $r^2=0.773$, $P<.001$, $F=58.01$, $y=83.76+16.07x$; (B) intraosseous-intra-articular-periarticular tophi, $r^2=0.670$, $P<.001$, $F=32.43$, $y=715.25+0.137x$; (C) intraosseous-intra-articular tophi, $r^2=0.410$, $P=.002$, $F=13.19$, $y=83.73+7.22x$. y =erosion volume, x =urate volume.

damage in gout. Another DECT study^[10] demonstrates that MSU crystals deposit outside the bone and contribute to bone erosion through an “outside-in” mechanism. Our study has expanded the observations to quantitatively analyze the direct role of MSU crystal components within the tophi in the formation of bone erosion by measuring urate volume and erosion volume. MSU crystal deposits presented within the joint, within bone erosion, and adjacent to joint, were separately analyzed in our study. We found that the relationships between MSU crystals within tophi and bone erosions were correlated to the anatomic location of urate deposition. The strongest positive correlation was demonstrated in intraosseous tophi and all positive correlations were demonstrated in those tophi that contained an intraosseous component.

We considered that erosion volume/urate volume could represent the erosion volume caused by the different tophi that had the same urate volume. Hence, it would indirectly reflect the effects of MSU crystals on promoting bone erosions in the respective tophi. For the intraosseous tophi, intraosseous-intra-articular tophi and intraosseous-intra-articular-periarticular tophi, the urate volume and erosion volume successively increased with the decrease of erosion volume/urate volume,

which indicated that the erosion volume, caused by the tophi, successively decrease when the urate volume was the same. All strongly positive correlations between urate volume and erosion volume were demonstrated in the mentioned tophi that contained an intraosseous component. The strongest positive correlation was demonstrated in the intraosseous tophi. The data indicated that MSU crystal deposition had varying degrees of effects on promoting the development of bone erosions, which was associated with the anatomic location of urate deposition in joints. Furthermore, urate deposition within erosion had the strongest effect to promote bone erosion. MSU crystal deposition was present primarily within the joint or on the surface of articular cartilage, which probably caused cartilage damage and allowed focal contact of MSU crystals with subchondral bone.^[7] This may further promote the development of erosion by inducing local production of cytokines, chemokines, and enzymes.^[21,22] It possibly is the dominant pathological mechanism responsible for bone erosions in tophi that contain an intraosseous component, which can be considered in the context of these imaging results.

Our data also showed that almost all erosion volumes were larger than urate volumes in nonperiarticular tophi, in contrast

with most erosion volumes less than urate volumes in tophi that contained a periarticular component. For the intra-articular tophi and intra-articular-periarticular tophi, excluding the influence of intraosseous tophi, the urate volume successively increased with the decrease of erosion volume and erosion volume/urate volume. The correlation between urate volume and erosion volume was mildly positive in the intra-articular tophi, compared with no significant correlation in the intra-articular-periarticular tophi. These results all suggested the effects of MSU crystals deposited adjacent to joints (promoting bone erosion) were significantly weakened, compared with the intraosseous tophi and intra-articular tophi. The erosive process in urate deposition that occurs within or adjacent to joints and occurs relatively far from the bone may be determined predominantly by the excessive osteoclastogenesis^[23] and the inhibition of osteoblast induced by MSU crystals^[24,25] (indirect pathway). MSU crystals that deposit outside of the joints may lack stromal cells, such as synovial fibroblasts, chondrocyte, and macrophages, which leads to the decreased stimulation of osteoclastogenesis; this may explain the image results of periarticular tophi. Individual periarticular tophus that is in contact with erosion was not presented in our study. We were unable to dissect the relationship between periarticular tophi and bone erosion.

For the nonintraosseous tophi, due to the existence of articular cartilage, contact with subchondral bone was restricted and bone erosions mainly developed through the indirect pathway, which was greatly weaker than the effects caused by MSU crystals directly eroding into the bone. Otherwise, 1 clinical study suggested that the addition of antiosteoclast therapy may not be more beneficial than urate-lowering therapy alone in people with longstanding and tophaceous gout, which may also emphasize the direct role of MSU crystals in the development of bone erosions in gout.^[26] One exploratory study suggested that profound urate lowering therapy (serum urate level <1 mg/dL) during pegloticase treatment can lead to improvement to the structural damage (particularly bone erosion) in tophaceous gout.^[27] These findings raise the possibility that the intraosseous tophi regression may be used to monitor the response to urate-lowering therapy. Further prospective studies are needed to determine what target serum urate is needed to be achieved for erosion repair caused by intraosseous tophi, compared with nonintraosseous tophi.

Moderate positive correlations were demonstrated between total urate burden and total erosions. The disease duration had a mild positive correlation with the total erosions. The number of tophi had mild to moderate positive correlations with the total urate burden and erosions. These results illustrated that a high level of urate burden increased the number of tophi and caused greater structural joint damage. These findings support the idea that early intensive urate-lowering therapy may have a major benefit to prevent or reverse structural joint damage in people with gout. In our study, almost all patients with chronic gout had long disease duration and some patients received varying degrees of urate-lowering therapy, which involved a wide range of serum urate concentrations at the time of scanning. This may explain why the total urate burden does not correlate with the serum uric acid level.

This analysis has some limitations: due to the limitations of DECT in the assessment of synovitis and bone marrow edema (BMO), further longitudinal studies are required to directly explore the influence of synovitis and BMO in gouty bone erosion. Otherwise, DECT does have limitations of detection, and very small urate deposits may not be detected using this

method.^[28] In nonintraosseous tophi, it is possible that previous remodeling of bone erosions, or urate deposits within erosions may occur following urate-lowering therapy, or that very small deposits of crystals on the surface of articular cartilage may cause false negatives when using DECT. We only analyzed the direct relationship between MSU crystals and bone erosions, but left out the corona zones and fibrovascular zones within the tophus. Further studies are required to separately analyze the role of MSU crystals and the chronic inflammatory tissue response to these crystals in the development of bone erosions. We also acknowledged that our study had a small sample size for the inclusion criteria of patients identified for the presence of urate in contact with bone erosion, which was relatively infrequent. Consistent with the epidemiology of gout, all of the subjects were men, and these findings were inability to generalize results to women.

5. Conclusion

This study demonstrates that MSU crystal deposition has a promoting effect on the development of bone erosions in varying degrees, which is associated with the anatomic location of MSU crystal deposition. The intraosseous tophi contribute the most to bone erosions, followed by intra-articular tophi, and periarticular tophi.

Acknowledgments

The authors thank the members of the Rheumatology and Radiology Departments of the Second Affiliated Hospital of Zhejiang University School of Medicine for providing patient information and valuable comments for the study.

Author contributions

Conceptualization: Dan Shi, Jie-Yu Chen, Hua-Xiang Wu, Qi-Jing Zhou, Hai-Yan Chen, Yuan-Fei Lu, Ri-Sheng Yu.

Data curation: Dan Shi, Jie-Yu Chen, Hua-Xiang Wu, Qi-Jing Zhou, Ri-Sheng Yu.

Formal analysis: Dan Shi, Jie-Yu Chen, Hua-Xiang Wu, Hai-Yan Chen, Yuan-Fei Lu, Ri-Sheng Yu.

Investigation: Dan Shi, Jie-Yu Chen, Qi-Jing Zhou, Hai-Yan Chen, Yuan-Fei Lu, Ri-Sheng Yu.

Methodology: Dan Shi, Jie-Yu Chen, Hua-Xiang Wu, Qi-Jing Zhou, Hai-Yan Chen, Yuan-Fei Lu, Ri-Sheng Yu.

Project administration: Dan Shi, Hua-Xiang Wu, Ri-Sheng Yu.

Software: Dan Shi, Jie-Yu Chen, Ri-Sheng Yu.

Supervision: Dan Shi, Hua-Xiang Wu, Ri-Sheng Yu.

Validation: Dan Shi, Ri-Sheng Yu.

Visualization: Dan Shi, Ri-Sheng Yu.

Writing – Original Draft: Dan Shi, Jie-Yu Chen, Hua-Xiang Wu, Qi-Jing Zhou, Hai-Yan Chen, Yuan-Fei Lu, Ri-Sheng Yu.

Writing – Review & Editing: Dan Shi, Jie-Yu Chen, Hua-Xiang Wu, Qi-Jing Zhou, Hai-Yan Chen, Yuan-Fei Lu, Ri-Sheng Yu.

Ri-Sheng Yu orcid: 0000-0003-0554-9484.

References

- [1] Zhu Y, Pandya BJ, Choi HK. Prevalence of gout and hyperuricemia in the US general population: the National Health and Nutrition Examination Survey 2007–2008. *Arthritis Rheum* 2011;63:3136–41.

- [2] Kuo CF, Grainge MJ, Zhang W, et al. Global epidemiology of gout: prevalence, incidence and risk factors. *Nat Rev Rheumatol* 2015; 11:649–62.
- [3] McQueen FM, Reeves Q, Dalbeth N. New insights into an old disease: advanced imaging in the diagnosis and management of gout. *Postgrad Med J* 2013;89:87–93.
- [4] Dalbeth N, Aati O, Gao A, et al. Assessment of tophus size: a comparison between physical measurement methods and dual-energy computed tomography scanning. *J Clin Rheumatol* 2012;18:23–7.
- [5] Hughes GR, Barnes CG, Mason RM. Bony ankylosis in gout. *Ann Rheum Dis* 1968;27:67–70.
- [6] Rasaratnam I, Christophidis N. Gout: 'a disease of plenty'. *Aust Fam Physician* 1995;24:849–51.
- [7] Sokoloff L. The pathology of gout. *Metabolism* 1957;6:230–43.
- [8] Dalbeth N, Clark B, Gregory K, et al. Mechanisms of bone erosion in gout: a quantitative analysis using plain radiography and computed tomography. *Ann Rheum Dis* 2009;68:1290–5.
- [9] Dalbeth N, Aati O, Kalluru R, et al. Relationship between structural joint damage and urate deposition in gout: a plain radiography and dual-energy CT study. *Ann Rheum Dis* 2015;74:1030–6.
- [10] Towiwat P, Doyle AJ, Gamble GD, et al. Urate crystal deposition and bone erosion in gout: 'inside-out' or 'outside-in'? A dual-energy computed tomography study. *Arthritis Res Ther* 2016;18:208.
- [11] McQueen FM, Doyle A, Reeves Q, et al. Bone erosions in patients with chronic gouty arthropathy are associated with tophi but not bone oedema or synovitis: new insights from a 3 T MRI study. *Rheumatology (Oxford)* 2014;53:95–103.
- [12] Thiele RG. Role of ultrasound and other advanced imaging in the diagnosis and management of gout. *Curr Rheumatol Rep* 2011;13:146–53.
- [13] Paparo F, Zampogna G, Fabbro E, et al. Imaging of tophi with an extremity-dedicated MRI system. *Clin Exp Rheumatol* 2011;29:519–26.
- [14] Choi HK, Al-Arfaj AM, Eftekhari A, et al. Dual energy computed tomography in tophaceous gout. *Ann Rheum Dis* 2009;68:1609–12.
- [15] Yu L, Primak AN, Liu X, McCollough CH. Image quality optimization and evaluation of linearly mixed images in dual-source, dual-energy CT. *Med Phys* 2009;36:1019–24.
- [16] Perry D, Stewart N, Benton N, et al. Detection of erosions in the rheumatoid hand; a comparative study of multidetector computerized tomography versus magnetic resonance scanning. *J Rheumatol* 2005; 32:256–67.
- [17] Dohn UM, Eijbjerg BJ, Hasselquist M, et al. Rheumatoid arthritis bone erosion volumes on CT and MRI: reliability and correlations with erosion scores on CT, MRI and radiography. *Ann Rheum Dis* 2007; 66:1388–92.
- [18] Wallace SL, Robinson H, Masi AT, et al. Preliminary criteria for the classification of the acute arthritis of primary gout. *Arthritis Rheum* 1977;20:895–900.
- [19] Shi D, Xu JX, Wu HX, et al. Methods of assessment of tophus and bone erosions in gout using dual-energy CT: reproducibility analysis. *Clin Rheumatol* 2015;34:755–65.
- [20] Schlesinger N, Thiele RG. The pathogenesis of bone erosions in gouty arthritis. *Ann Rheum Dis* 2010;69:1907–12.
- [21] Cunningham CC, Corr EM, McCarthy GM, et al. Intra-articular basic calcium phosphate and monosodium urate crystals inhibit anti-osteoclastogenic cytokine signalling. *Osteoarthritis Cartilage* 2016; 24:2141–52.
- [22] Dalbeth N, Pool B, Gamble GD, et al. Cellular characterization of the gouty tophus: a quantitative analysis. *Arthritis Rheum* 2010; 62:1549–56.
- [23] Dalbeth N, Smith T, Nicolson B, et al. Enhanced osteoclastogenesis in patients with tophaceous gout: urate crystals promote osteoclast development through interactions with stromal cells. *Arthritis Rheum* 2008;58:1854–65.
- [24] Chhana A, Callon KE, Pool B, et al. Monosodium urate monohydrate crystals inhibit osteoblast viability and function: implications for development of bone erosion in gout. *Ann Rheum Dis* 2011;70:1684–91.
- [25] Bouchard L, de Medicis R, Lussier A, et al. Inflammatory microcrystals alter the functional phenotype of human osteoblast-like cells in vitro: synergism with IL-1 to overexpress cyclooxygenase-2. *J Immunol* 2002;168:5310–7.
- [26] Dalbeth N, Aati O, Gamble GD, et al. Zoledronate for prevention of bone erosion in tophaceous gout: a randomised, double-blind, placebo-controlled trial. *Ann Rheum Dis* 2014;73:1044–51.
- [27] Dalbeth N, Doyle AJ, McQueen FM, et al. Exploratory study of radiographic change in patients with tophaceous gout treated with intensive urate-lowering therapy. *Arthritis Care Res (Hoboken)* 2014;66:82–5.
- [28] Melzer R, Pauli C, Treumann T, Krauss B. Gout tophus detection: a comparison of dual-energy CT (DECT) and histology. *Semin Arthritis Rheum* 2014;43:662–5.